Results in Physics 12 (2019) 2206–2212

Contents lists available at ScienceDirect

Results in Physics

journal homepage: www.elsevier.com/locate/rinp

Influences of substrate pretreatments and Ti/Cr interlayers on the adhesion and hardness of CrAlSiN and TiAlSiN films deposited on Al_2O_3 and ZrO_2-$8Y_2O_3$ thermal barrier coatings

Wolfgang Tillmann, Alexander Fehr*, Dominic Stangier, Markus Dildrop

Institute of Materials Engineering, TU Dortmund University, 44227 Dortmund, Leonhard-Euler-Str. 2, Germany

ARTICLE INFO

Keywords:
Duplex coating
Thermal barrier coating
CrAlSiN
TiAlSiN
Coating adhesion
Microhardness

ABSTRACT

Using atmospheric plasma spraying (APS), ceramic Al_2O_3 and ZrO_2-$8Y_2O_3$ thermal barrier coatings (TBC) were applied on AISI H11 (1.2343) and subsequently polished to serve as a substrate to magnetron sputter $CrAlSi_{7.5}N$ and $TiAlSi_{7.9}N$ films. The influences of polishing as well as plasma etching processes on the surface roughness and residual stresses of the TBCs were correlated with the adhesion of the metal nitride films. As metallic interlayers are typically used to metallize insulating substrates to increase the film adhesion, the effect of different Cr and Ti interlayer thicknesses (50–150 nm) on the $CrAlSi_{7.5}N$ and $TiAlSi_{7.9}N$ adhesion was examined. Despite tensile stresses in the TBCs, a duplex coating structure, consisting of Al_2O_3 + $Ti_{100\ nm}$/$TiAlSi_{7.9}N$, generated a high adhesion (L_{c3} = 61.04 ± 2.36 N). In contrast to Cr, titanium interlayers are assumed to lead to a stress relaxation in the interface between the TBC and the PVD film. In general, using ZrO_2-$8Y_2O_3$ as a substrate resulted in a minor adhesion of all PVD film combinations, which is traced back to lattice mismatches between the substrate and the films. Moreover, the number of pores on the TBC surface is crucial for the adhesion and hardness of $CrAlSi_{7.5}N$ and $TiAlSi_{7.9}N$.

Introduction

To counter the complex stress profile of cutting and forming tools, coating process combinations of thermal spraying (TS) and physical vapor deposition (PVD) enable to unite characteristic coating properties, i.e. thermal insulation as well as wear protection, for instance, which cannot be obtained by the sole coating processes. If the substrate hardness is significantly lower than that of the film, PVD coatings with low film thicknesses (< 10 µm) will reach the limits of their mechanical properties when the films are exposed to increased contact stresses. In this case, so called duplex coatings that combine the above mentioned coating types can benefit the adaption of the hardness gradient between the substrate and the film [1]. One of the main challenges when combining dissimilar coating types, however, is to achieve good PVD film adhesions. As TS processes generate relatively rough surfaces, post-treatments, such as polishing procedures, are necessary to generate smooth surfaces for the deposition of PVD nitride films [1,2]. Furthermore, *Kobayashi* et al. revealed that thicker atmospheric plasma sprayed (APS) zirconia coatings significantly enhance the adhesion of DLC films. They assumed that the lower porosity and higher hardness of thicker TS coatings are responsible for the increased film adhesion within a zirconia coating thickness variation (65–210 µm) [3]. While most studies focus on duplex structures of cemented carbides like WC-Co and metal nitride PVD coatings [1,2,4–7], the state of knowledge concerning PVD metal nitride depositions on ceramic substrates is still fairly limited. Instead, several studies rather focus on a metallization of ceramics. Nickel films, for instance, can establish Ni oxides on ZrO_2-$9Y_2O_3$ due to an oxygen ion (O^{2-}) interchange, which is promoted merely at elevated temperatures (600 K) [8]. *Munoz* et al. identify discrepancies in the lattice parameters and the electronic properties as a major obstacle for metal-zirconia interfaces [9]. Thus, new approaches are required to foster the adhesion properties of metal nitride films on oxide ceramics, such as Al_2O_3 or yttrium-stabilized zirconia (YSZ).

Two methods that enable to increase the PVD film adhesion are plasma assisted metal or gas ion etching of the substrates prior to the film deposition [10]. *Ehiasarian* et al. showed that metal ion etching allows to implant metal ions in high speed and stainless steel substrate surfaces, which results in increased critical loads of CrN films (L_{c3} = 85 N) [11]. The integration of metal ions into depths of up to 10 nm into the substrate is further accompanied by a 100 nm substrate

* Corresponding author.
E-mail addresses: wolfgang.tillmann@tu-dortmund.de (W. Tillmann), alexander.fehr@tu-dortmund.de (A. Fehr), dominic.stangier@tu-dortmund.de (D. Stangier), markus.dildrop@tu-dortmund.de (M. Dildrop).

https://doi.org/10.1016/j.rinp.2019.02.048
Received 13 February 2019; Accepted 15 February 2019
Available online 20 February 2019

material removal [12]. Gas ion etching utilizing Ar or H_2 helps to remove contaminants and oxides on the substrate surface, leading to an increased surface roughness that fosters the film adhesion [13]. Combined gas and metal ion etching processes contribute in particular to an epitaxial growth and improved adhesion of the coating [14].

A further approach to increase the adhesion of PVD films on TS-coated substrates, is the deposition of a metallic interlayer (e.g. titanium), which results in minor residual stress gradients in the transition zone. Thus, the idea is to generate a strong chemical bond with an increased ductility, which can withstand external shear stresses [2,15]. Interlayers such as titanium can further dissolve oxide contaminants at the surface of the substrate [13]. Typically, the internal stresses of nitride PVD films are absorbed by 0.5–1.5 µm thick metallic films [2,16]. Increasing interlayer thicknesses, however, cause a decrease of the hardness and wear resistance of PVD coating structures [17].

While the majority of the initially mentioned studies refer to duplex coatings of cemented carbides like WC-Co and metal nitride PVD films, approaches to increase the PVD film adhesion on ceramic substrates are not yet thoroughly investigated. Thus, two different coating systems that integrate an APS thermal barrier coating (TBC), i.e. Al_2O_3 or ZrO_2-$8Y_2O_3$ and a magnetron sputtered film ($CrAlSi_{7.5}N$ or $TiAlSi_{7.9}N$) applied on an AISI H11 (1.2343) steel substrate, will be prepared. Since decreasing the TS surface roughness is inevitable for a subsequent PVD film deposition, the influence of intermediate TS coating treatments, i.e. polishing and plasma etching, on the surface roughness and the residual stresses of the substrates will be scrutinized. In addition, it will be examined how the thickness of Cr and Ti interlayers affects the adhesion of $CrAlSi_{7.5}N$ and $TiAlSi_{7.9}N$. Finally, the effects of the TBC substrate pretreatments will be correlated with the adhesion and the hardness of $CrAlSi_{7.5}N$ and $TiAlSi_{7.9}N$.

Experimental

Material and substrate pretreatments

For the deposition of both the TS as well as the PVD coatings, a hot work steel AISI H11 (1.2343) was used as a substrate material. The chemical composition of this steel is summarized in Table 1. The steel substrates had had a 40 mm diameter and a thickness of 4 mm. The TS substrates were merely solution annealed and not heat-treated due to the self-supporting characteristics of the TS coatings. For the deposition of PVD monolayer coatings, which served as a reference, steel substrates were polished and plasma nitrided to generate a gradient hardness profile. The nitriding process was conducted in an Arc-PVD device (Type PVD20, Co. Metaplas, Germany). The nitriding time was 8 h and the substrate temperature was kept constant at 650 °C. Plasma nitriding was performed with a pressure of 2 mbar and a bias voltage of U = −650 V, while a H_2:N_2 gas ratio of 3:1 was set. Based on previous investigations [18], this approach resulted in a hardness increase from 3 to up to 11 GPa.

Thermal spray process

Prior to the TS coating procedure, the round, unprepared samples were grit blasted with a blasting angle of 45° and with a stand-off distance of 100 mm. As blasting material, corundum (EKF 24) with a grain size of 600–850 µm was utilized to obtain an increased surface roughness of approximately Rz = 30 µm.

All TS coatings were manufactured by APS using a plasma gun F4-MB, Oerlikon Metco, Switzerland. The spray powders were radially injected into the plasma flame in an 90° angle, using argon as a carrier gas. Prior to the application of alumina and zirconia coatings, a metallic NiCoCrAlHfYSi bonding agent (Amdry 997, Oerlikon Metco, −38 + 5 µm) was applied. For the spraying of alumina and zirconia coatings, Metco 6051, −31 + 5.5 µm as well as Metco 204F, −45 + 15 µm feedstocks, both from Oerlikon Metco, were utilized. The corresponding APS parameters for all TS coatings are listed in Table 2. Since the applied TBCs exhibited an increased surface roughness in the as-sprayed state, grinding and polishing procedures with a maximum polishing level of 1 µm were necessary to generate smooth surfaces, enabling the subsequent deposition of near-net shaped PVD films onto the TS coatings.

Table 1
Chemical composition (wt%) of AISI H11 (1.2343) X38CrMoV5-1.

C	Si	Mn	P	S	Cr	Mo	V
0.36–0.42	0.9–1.2	0.3–0.5	≤0.3	≤0.03	4.8–5.5	1.1–1.4	0.25–0.5

Table 2
Feedstocks and corresponding APS parameters.

	NiCoCrAlHfYSi bonding agent	Al_2O_3	ZrO_2-$8Y_2O_3$
Current [A]	600	600	600
Ar [slpm]	65	44	44
H_2 [slpm]	8	13	13
Ar carrier gas [slpm]	1.9	2.8	2.8
Injector diameter [mm]	1.5	1.8	1.8
Injector angle [°]	70	90	90
Track pitch [mm]	4	2	2
Spray distance [mm]	145	130	130

PVD coating process

In order to investigate the influence of a TS coating, which is applied underneath a PVD coating, on the adhesion, $CrAlSi_{7.5}N$ and $TiAlSi_{7.9}N$ thin films were deposited on pure plasma nitrided metallic AISI H11 (1.2343) substrates as well as on post-treated TS coatings. Furthermore, two different metallic interlayers (Ti and Cr) with varying thicknesses (50–150 nm) were applied between the TBCs and the metal nitride films to analyze the influence of the interlayer thickness on the adhesion properties.

PVD films were deposited using a magnetron sputtering (MS) device (CC800/Custom ML, Cemecon, Germany) equipped with four unbalanced planar magnetron sources. For the deposition of $CrAlSi_{7.5}N$, two AlCr24 plug targets as well as a monolithic Cr target, and a Si target were utilized. Two TiAl60 plug targets, a monolithic Ti target, and a Si target, were employed as sputter materials to synthesize $TiAlSi_{7.5}N$.

Prior to the PVD coating deposition of $CrAlSi_{7.5}N$ and $TiAlSi_{7.9}N$, the polished steel and APS coated samples were cleaned for 15 min in an ultrasonic ethanol bath. After drying and positioning the samples in the magnetron sputtering (MS) device, two heating processes (8.8 kW) were carried out with an initial pressure of 10 mPa. Gas ion etching (GIE) by means of argon and krypton noble gas and metal ion etching (MIE) were performed to clean the substrate and target surfaces, removing oxides that inhibit the adhesion [10,13,19]. The GIE plasma treatment was conducted for 25 min, using a MF pulsed bias voltage of −650 V at a frequency of 250 kHz, controlled by an argon/krypton pressure of 350 mPa. The MIE process was performed with CrAl24 and TiAl60 targets, respectively, applying a constant power of 2 kW for 1 h. Furthermore, a bias voltage of −200 V was applied on the substrates and an argon gas flow of 240 mln as well as a krypton gas flow of 180 mln were set. Afterwards, the influence of this two-staged plasma etching process on the surface roughness of the substrates was investigated.

The MS-PVD process parameter sets for the synthesis of $CrAlSi_{7.5}N$ and $TiAlSi_{7.9}N$ are listed in Table 3. Within this context, krypton was applied to increase the ionization rate. The deposition parameters are based on a previous study [18] to correlate the coating adhesion on steel and TBC substrates. For the deposition of metallic Cr and Ti interlayers, a constant cathode power of 4 kW was set and the layer thickness was varied between 50 and 150 nm.

Table 3
PVD process parameters for the deposition of CrAlSiN and TiAlSiN.

	CrAlSiN	TiAlSiN
2 × TiAl60 [kW]	–	9.5
2 × AlCr24 [kW]	5.0	–
Ti [kW]	–	2.0
Cr [kW]	1.0	–
Si [kW]	2.0	3.0
DC Bias [V]	−120.0	−100.0
Ar/Kr ratio	1	1.5
N_2 controller [mPa]	500.0	580.0
Chamber temperature [°C]	~600.0	~700.0

Characterization of the TBCs and the applied PVD films

A light microscope was utilized to analyze the morphology and to determine the porosity of the thermally sprayed TBCs. For the evaluation of the TBC surface roughness in the as-sprayed as well as in the polished and the plasma etched state, an optical 3D-surface analyzer (Infinite Focus, Alicona, Austria) was employed. The hardness of the ceramic TBCs was determined by means of a small load hardness testing device (Type M 400, Co. Leco, Germany) with a test load of HV0.1. The residual stress state of the different substrates was analyzed by means of a diffractometer Type D8 Advance (Bruker, Germany), using the $\sin^2\psi$ method to determine changes of the lattice plane distances (d). As a radiation source, Fe-Kα with a wave length of 0.194 nm, working at a voltage of 30 kV and with a current of 28 mA was utilized. The sample tilts were varied between $\psi = 0$ and 60° and rotated for $\Phi = 0°$, 90°, 180°, and 270° using steps of $\Delta\theta = 0.15°$. The evaluated 2θ peaks as well as the X-ray elastic constants, which were calculated according to *Kröner* [15], are given in Table 4.

The morphologies of the PVD films were analyzed with a field emission scanning electron microscope (SEM) (FE-JSEM 7001F, Jeol, Japan). Prior to the SEM investigations, the duplex coatings were prepared by means of a cross-section polisher IB-09010CP, Jeol, to generate smooth cross-sections with minimal deformations.

The microhardness of the $CrAlSi_{7.5}N$ and $TiAlSi_{7.9}N$ thin films were determined using a nanoindenter G200 Agilent Technology, USA, which is equipped with a Berkovich diamond tip. The investigation was based on the study of *Oliver* et al. [16] and includes 49 indentations with a distance of 50 µm in a square array of 7 × 7. Furthermore, to exclude hardness effects of the metallic substrates and the TS coatings, the hardness values were only evaluated for 10% of the entire PVD coating thickness. In addition, a constant Poisson's ratio of 0.25 was assumed for the evaluation of the hardness values. The adhesion strength of the metal nitride films was investigated by means of a scratch test Revetest (CSM Instruments, Switzerland). This method is based on the ASTM standard method to determine the adhesion strength [17] and works with a Rockwell-C diamond tip, which is scratched with a linearly increasing force of up to 100 N for 10 mm at a velocity of 10 mm/min over the coated surface. Although the ASTM guideline [17] stipulates the use of a diamond stylus with a 200 µm tip radius, a tip with r = 100 µm was used for the scratch tests. Based on previous works [11], this sharper tip was utilized since the adhesion of $TiAlSi_{7.9}N$, deposited on nitrided AISI H11 (1.2343) steel, did not exhibit any spallation after the scratch test when using a r = 200 µm tip. For a precise determination of the critical loads (L_{c3}) of $CrAlSi_{7.5}N$ and $TiAlSi_{7.9}N$, scanning electron microscopy was employed.

Results and discussion

The morphology, surface roughness, and hardness of the TBCs were investigated to later correlate these properties with the adhesion of PVD films. In this context, the effects of polishing and plasma etching treatments of the TBCs were of particular interest. Subsequently, the adhesive properties of the applied $CrAlSi_{7.5}N$ and $TiAlSi_{7.9}N$ films with respect to the Cr and Ti interlayers were evaluated and related to the topography as well as the stress state of the TBCs.

Analyses and pretreatments of the ceramic substrates

The morphology of the Al_2O_3 and ZrO_2-$8Y_2O_3$ APS coatings is visualized in Fig. 1. Similar coating thicknesses were obtained for both TBC structures. The NiCoCrAlHfYSi bonding agent had a thickness of approximately 100 µm while the coating thicknesses of the TBCs varied between 500 and 600 µm in the as-sprayed state. These high coating thicknesses, in comparison to conventional APS coatings, were required in order to decrease the surface roughness by grinding and polishing for the subsequent PVD coating application. The Al_2O_3 coating resulted in a porosity of 9 ± 1.2%, whereas the zirconia coating exhibited a slightly higher porosity (12 ± 1.45%) due to the coarser particle size. The surface roughness of the TBCs in the as-sprayed state both exhibited an Rz value of approximately 24.75 µm. Grinding and polishing resulted in a clearly decreased surface roughness (Rz < 1 µm) compared to the as-sprayed state (see Fig. 2). Although *Kobayashi* et al. state that higher TS thicknesses result in a lower porosity [3], the experiments revealed that the mechanical pretreatment opened initially closed pores at the TBC surfaces. Similar to the TBC porosity, the hardness of alumina was 972 ± 55 HV0.1 whereas the hardness of ZrO_2-$8Y_2O_3$ was 838 ± 103 HV0.1, since denser coating structures contribute to an increased coating hardness [20,21].

The influence of a plasma etching process, which combined gas and metal ion etching, on the surface roughness of polished TBCs is illustrated in Fig. 3. In general, plasma etching slightly increased the roughness compared to the substrates in the polished state, since a material removal takes place [10,13,14]. The etching process was most significant for the steel substrates, while the surface roughening effect was negligible for the TBC substrates. The rougher steel substrates could be traced back to a higher amount of metal ions being integrated into the surfaces of the substrate [12].

The influence of the different substrate pretreatments on the residual stress state was analyzed as well. Fig. 4 indicates compressive stresses of the AISI H11 (1.2343) substrate in its initial and post-treated state. Especially polishing and nitriding, as well as plasma etching [22], resulted in a considerable increase of compressive stresses in the steel substrates. The nitriding process caused a hardness increase of the steel substrates, as nitrogen dissolves into the iron lattice, leading to precipitation hardening and solid solution hardening [23]. Due to nitrogen diffusions into the steel surface, compressive stresses were increased. In particular, the increased Cr, Mo, and V contents in AISI H11 (cf. Table 1) contributed to a nitride formation. Due to the embedment of nitrogen in the iron lattice structure, the lattice is distorted [24,25], thus inducing increased compressive stresses (−720 ± 10.1 MPa). In contrast to this, a subsequent plasma etching process decreased the

Table 4
X-ray elastic constants (XEC) of the AISI H11 substrate and the TBCs.

Material	2 Θ [°]	(*h k l*)	Poisson ratio	Young's modulus [MPa]	s_1 [10^{-6} MPa^{-1}]	$1/2s_2$ [10^{-6} MPa^{-1}]
Ferrite	145.56	220	0.28	220,264	−1.271	5.811
γ-Al_2O_3	89.60	300	0.23	408,163	−5.635	3.014
ZrO_2-$8Y_2O_3$	77.42	311	0.31	240,385	−1.29	5.45

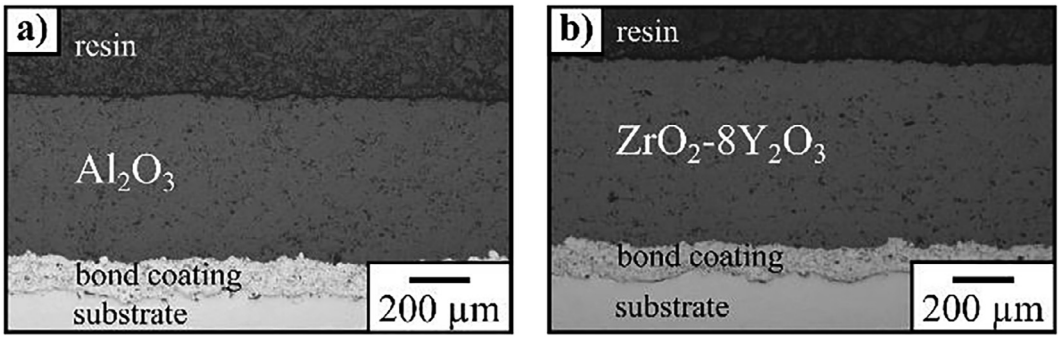

Fig. 1. Morphology of a) Al_2O_3 and b) ZrO_2-$8Y_2O_3$ APS coatings.

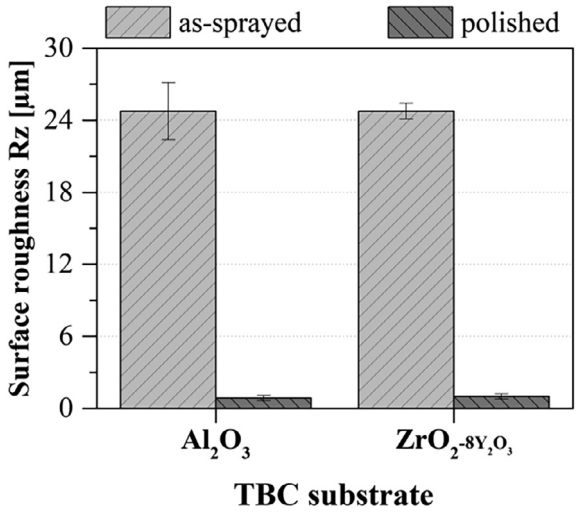

Fig. 2. Surface roughness states of TBCs before and after pretreatments.

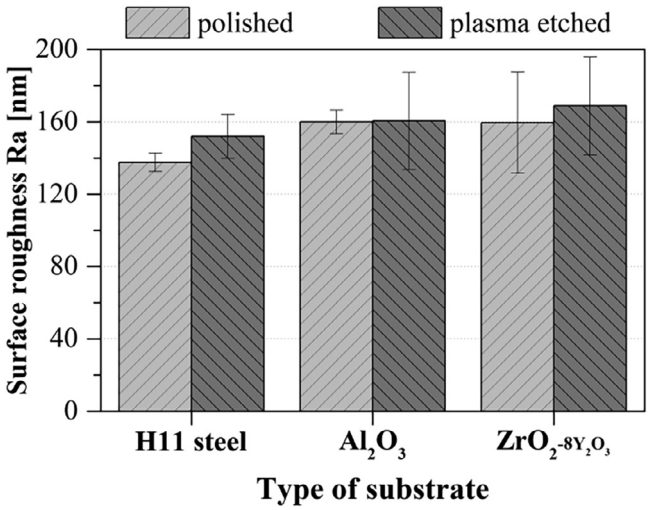

Fig. 3. Influence of plasma etching on the surface roughness of steel and TBCs.

compressive stresses to a value of -423.8 ± 6.1 MPa. This behavior can be explained by the fact that plasma etching provides an energy influx into the steel, accompanied by heat, thereby transforming some compressive stresses into tensile stresses [26]. Furthermore, the two heating processes prior to the etching process had a similar effect as the heat treatment, leading to a lattice relaxation of the substrate. Compared to the pure steel substrates, the entire thermally sprayed Al_2O_3 and ZrO_2-$8Y_2O_3$ substrates exhibited tensile stresses of up to 610 ± 10.3 MPa (Fig. 4). Moreover, polishing and plasma etching of

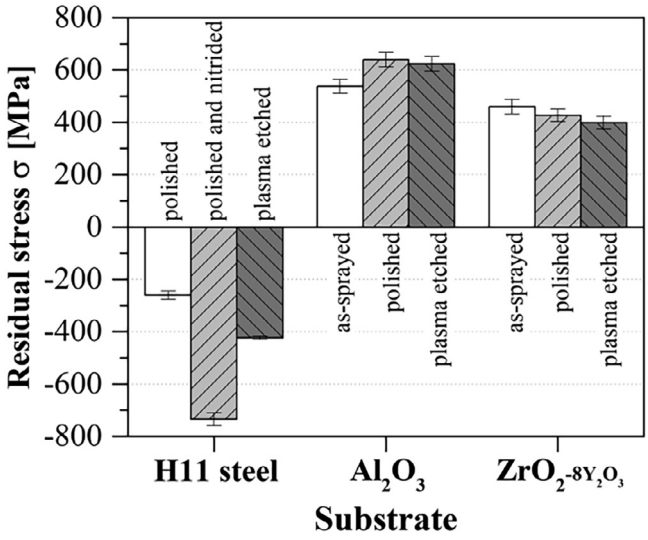

Fig. 4. Influence of steel and TBC substrate pretreatments on the residual stresses.

the TBCs did not have a great impact on the stress state. However, the tensile stresses of ZrO_2-$8Y_2O_3$ coatings were slightly lower than those of Al_2O_3, which corresponds with the porosity state of the TS coatings. Since the porosity of ZrO_2-$8Y_2O_3$ was ~3% higher compared to Al_2O_3, the residual stresses were 100–200 MPa lower [27].

In conclusion, polishing was necessary to decrease the surface roughness of the TBCs in the as-sprayed state. Since no substantial influence of plasma etching on the TBC surface roughness and the residual stresses could be revealed, this surface pretreatment was excluded from further analyses. The predominant tensile stresses in the TBCs, however, might have a substantial impact on the adhesion behavior of the metal nitride films, which were applied in the next step.

Adhesion and hardness of PVD films applied onto TBCs

Cr and Ti interlayers with varying thicknesses (0–150 nm) were deposited to analyze the influence of their thickness on the film adhesion of the $CrAlSi_{7.5}N$ and $TiAlSi_{7.9}N$ top films, which had a constant coating thickness of 2.5 µm.

Fig. 5(a) shows a $Ti_{100\ nm}$/$TiAlSi_{7.9}N$ system deposited on Al_2O_3. The nitride film exhibited a homogenous and densely grown structure, which is typical for the associated nanocomposite structure [28]. The image further shows that $TiAlSi_{7.9}N$ uniformly covered concave TBC surface cavities, which were exposed by the polishing treatment. In this context, *Mattox* states that a polishing process of brittle substrates can lead to cracks on the surfaces, which have a negative influence on the adhesion of the film [29]. Although the adherence of $TiAlSi_{7.9}N$ appeared to be sufficient in the pore, layer growth defects occurred at the

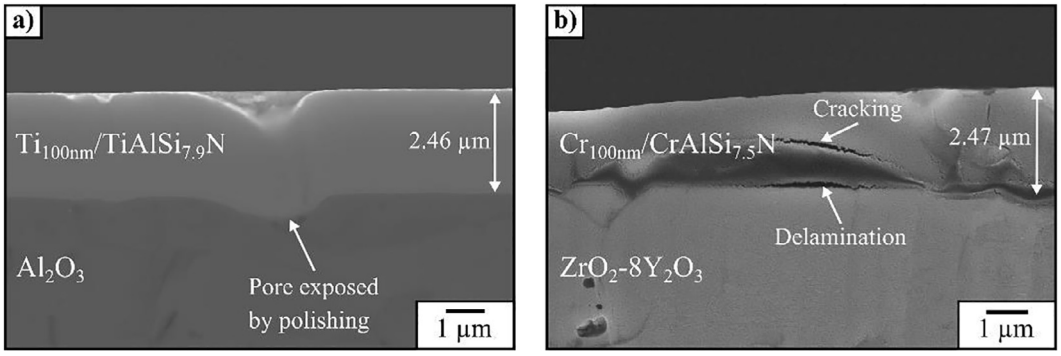

Fig. 5. Morphology of PVD films deposited on polished TBCs, a) $Ti_{100\ nm}/TiAlSi_{7.9}N$ on Al_2O_3, b) $Cr_{100\ nm}/CrAlSi_{7.5}N$ on ZrO_2-$8Y_2O_3$.

surface of the PVD layer. The development of cavities at the surface of the PVD film is assumed to negatively affect the mechanical as well as wear properties of the duplex coating system as these voids constitute a susceptibility for adhesive wear. Furthermore, local coating thickness irregularities are suspected to have a negative influence on the mechanical properties such as the hardness.

A duplex coating system of ZrO_2-$8Y_2O_3$ + $Cr_{100\ nm}/CrAl_{7.5}N$ is shown in Fig. 5(b), indicating that wide-open pores at the TBC surface result in a defective growth and even in a delamination of the nitride film [29]. Apart from that, the film also delaminated in flat polished regions, as indicated in the figure. Thus, in general, a low adhesion of the chromium-based PVD system on ZrO_2-$8Y_2O_3$, which is accompanied by cracks in the $CrAlSi_{7.5}N$ top film, could be assumed. A precise analysis of the PVD film adhesion with respect to the effect of the metallic interlayer thickness, is given in the following.

Effects of the interlayer thickness on the film adhesion

The critical loads (L_{c3}), which explained the failure of the $CrAlSi_{7.5}N$ and $TiAlSi_{7.9}N$ top films applied on steel and TBCs in dependence of the Cr/Ti interlayer thickness, are shown in Fig. 6. The graphic indicates that applying $CrAlSi_{7.9}N$ sans a Cr interlayer on steel or ceramic substrates resulted in considerably diverging film adhesions. Using a nitrided steel substrate lead to a L_{c3} value of 14.93 ± 1.03 N. In contrast, the $CrAlSi_{7.5}N$ film adhesion on the Al_2O_3 substrate was even higher (31.86 ± 2.08 N), while direct flaking was revealed on zirconia substrates. One explanation for these different adhesion behaviors of $CrAlSi_{7.5}N$ are varying lattice mismatches between the film and the different substrates [30]. Minor lattice mismatches between the coating and substrate, as supposed between $CrAlSi_{7.5}N$ and Al_2O_3, are beneficial to decrease stresses in the interface zone [31] and to finally increase the coating adhesion. Furthermore, differences in the thermal expansion coefficients of the substrate and the coating can result in a delamination of PVD films [15]. As the thermal expansion behavior of yttrium-stabilized zirconia ($12{\cdot}10^{-6}$/°C) is higher than of alumina ($8{\cdot}10^{-6}$/°C), increased residual stresses were induced, while the substrate cooled down after the sputtering process [32]. These heat-induced stresses, in turn, affected the PVD film adhesion.

The introduction of a 50–150 nm Cr interlayer between the steel and $CrAlSi_{7.5}N$ resulted in a slight increase of the film adhesion [33–35], which can be attributed to the small lattice mismatch between α-iron (a = 2.868 Å) and chromium (a = 2.871 Å). Compared to the steel substrates, relatively low to no adhesion was obtained by the application of Cr interlayers between the TBC substrates and $CrAlSi_{7.5}N$. For example, $Cr_{50\text{-}150\ nm}/CrAlSi_{7.5}N$, deposited on zirconia, resulted in a constant critical load of 6.85 ± 1.57 N (Fig. 6), which was independent of the interlayer thickness. This low adhesion can be explained by the fact that the Cr-based films exhibited delamination and cracking effects immediately after the deposition on zirconia TBCs as indicated in Fig. 5(b). A further explanation is the fact that chromium does not have as high affinity to ceramic oxides as to an iron-based substrate, since the lattice systems of the ceramic substrates differ considerably from that of cubic metals. Especially the tetragonal character of zirconia diverges from the structure of the chromium lattice, which results in low adhesion properties [9]. In this context, the ion interchange between the metallic film and the ceramic substrate and the resulting adhesion force could have been enhanced when annealing at increased temperatures, such as 600 K [8]. In addition, *Pawel* et al. assume that an ion beam

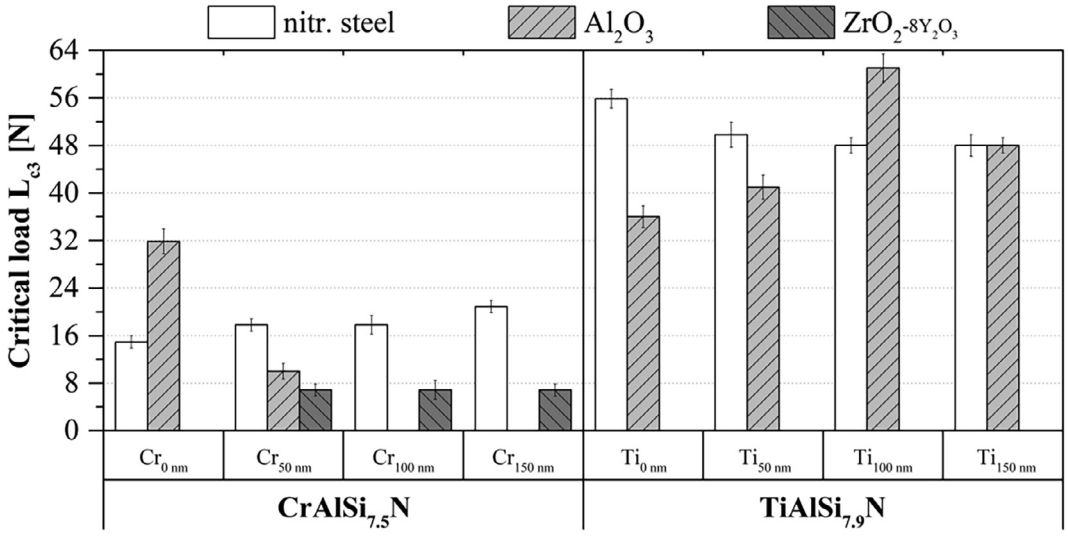

Fig. 6. Influence of the Cr/Ti interlayer thickness on the critical loads (L_{c3}) of $CrAlSi_{7.5}N$ and $TiAlSi_{7.9}N$ on nitrided steel and TBC substrates.

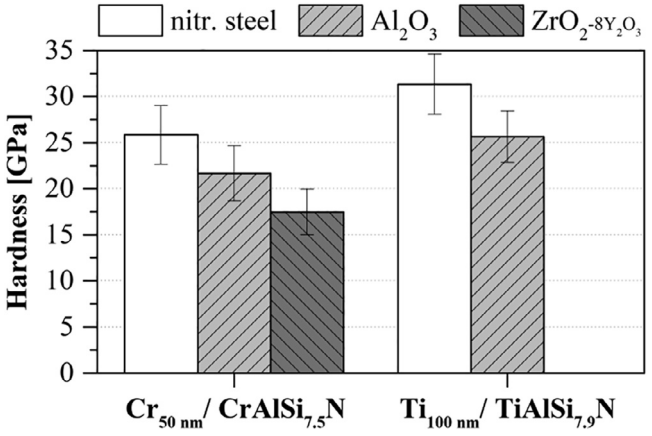

Fig. 7. Microhardness of $CrAlSi_{7.5}N$ and $TiAlSi_{7.9}N$, deposited on steel and TBC substrates.

mixing process supports an interchange of Cr and Al atoms in an Al_2O_3/Cr interface [36].

When the Cr interlayer thickness on alumina was increased to 100–150 nm, the adhesion of Cr/$CrAlSi_{7.5}N$ was no longer ensured. The reason for this development of delaminations is that with an increase of the Cr interlayer thickness, fractures are more likely to occur in the interface zone, if the coating system is subjected to shear forces [34,37]. This was the case in the scratch test. In contrast to the alumina substrates, the application of a 50–150 nm Cr interlayer helped to increase the adhesion of Cr/$CrAlSi_{7.5}N$ on zirconia substrates. Nonetheless, with regard to the adhesion, the residual stress state in the substrate has to be further considered. As the tensile stresses in the polished zirconia were lower than in the alumina substrates (cf. Fig. 4), there was a lower stress gradient in the interface zone between the substrate and the compressive stress-afflicted, sputtered films. This leads to the conclusion that increased tensile stresses affect the $CrAlSi_{7.5}N$ adhesion with an increasing Cr interlayer thickness.

Fig. 6 further shows the L_{c3} values for the $TiAlSi_{7.9}N$ coatings deposited on nitrided steel and on polished TBCs. The introduction of metallic Ti interlayers (50–150 nm) had no significant influence on the adhesion behavior of $TiAlSi_{7.9}N$ on nitrided steel. Other studies, however, state that the thickness of the Ti interlayer, deposited between an oxidized steel substrate and a TiN PVD film, is significant for the adhesion [17,38]. *Pischow* et al. assume that the film adhesion depends on the thickness of the oxide layer on the substrate and the thickness of the Ti interlayer, eventually leading to high titanium diffusion rates into the oxide [38]. Correlating this finding with the results of this study, a Ti interlayer thickness of 100 nm deposited on polished Al_2O_3 generated the highest $TiAlSi_{7.9}N$ adhesion (L_{c3} = 61.04 ± 2.36 N), which can be traced back to an exchange of Ti and oxide ions. The good adhesion properties are evidenced in Fig. 5(a), indicating that the near-net shaped $Ti_{100\ nm}$/$TiAlSi_{7.9}N$ system covered pores close to the surface of the alumina substrate. The fact that a Ti interlayer of 100 nm resulted in the highest adhesion of $TiAlSi_{7.9}N$ can be correlated with the works of *Kim* et al., who demonstrated via impact adhesion tests that cracks and indentation cavity volumes of a TiN film were significantly reduced with an increasing Ti interlayer thickness, as titanium absorbs the impact energies [17]. The adhesion enhancing effect of a Ti interlayer [38–41] can be further traced back to stress relaxations in the coating interface [2] and the induction of low compressive stresses [42], which is especially of important for Ti/$TiAlSi_{7.9}N$ depositions on tensile stress-afflicted Al_2O_3 (cf. Fig. 4). Here, it became evident that the titanium interlayer can compensate tensile stresses, which predominated in the Al_2O_3 substrate as well as compressive stresses of the steel substrate. When the Ti interlayer thickness on Al_2O_3 reached a certain value (100 nm), the adhesion on Al_2O_3 was even higher than on steel. However, no adhesion of $Ti_{0–150\ nm}$/$TiAlSi_{7.9}N$ on zirconia could be ascertained, since direct spallation effects occurred in the scratch test. This result is in compliance with the findings of *Yang* et al., who determined the adhesive strength of plasma sprayed ZrO_2-$3Y_2O_3$ on titanium substrates. The ceramic layers delaminated completely during the adhesive strength tests and exhibited a poorer adhesion when compared to ZrO_2-$4CeO_2$ on Ti substrates. It was assumed that the different tetragonal grain sizes in ZrO_2-$4CeO_2$ and ZrO_2-$3Y_2O_3$ are significant for the adhesive strength [43]. With regard to this investigation, the amount as well as the stoichiometry of the stabilizing oxides seem to have a significant impact on the adhesion properties of Ti on the stabilized zirconia. Compared to *Yang* et al., this study considered fully stabilized zirconia with 8% Y_2O_3, which is supposed to have a greater influence on the stability and the grain size of the tetragonal lattice. Due to the higher amount of the stabilization agent, an increased stability of the tetragonal phase is achieved [44], which is believed to influence the adhesion of PVD films.

In general, the $TiAlSi_{7.9}N$ films had a higher adhesion on steel and Al_2O_3 substrates than the $CrAlSi_{7.5}N$ films. This increased adhesion was supported by the application of a Ti interlayer, which compensated compressive as well as tensile stresses of the substrate. The stress relaxation behavior of Ti interlayers on steel and alumina was significantly more pronounced than compared to Cr interlayers. Although polishing of Al_2O_3 resulted in higher tensile stresses than zirconia (610 ± 10.3 MPa), the Ti/$TiAlSi_{7.9}N$ system exhibited a significantly higher film adhesion. The stress state in the ZrO_2-$8Y_2O_3$ substrates was rather insignificant for the PVD film adhesion as differences of the lattice structure prevailed between the substrate and the films, which result in low diffusion processes and marginal to no adhesion of $CrAlSi_{7.5}N$ and $TiAlSi_{7.5}N$.

Hardness of the PVD films

According to the scratch tests, only the $Cr_{50\ nm}$/$CrAlSi_{7.5}N$ and $Ti_{100\ nm}$/$TiAlSi_{7.9}N$ systems, which exhibited a sufficient adhesion on all utilized substrates, were considered and analyzed concerning their microhardness. Fig. 7 indicates that using nitrided steel as a substrate resulted in the highest hardness values for both nitride films when compared to depositions on Al_2O_3 or ZrO_2-$8Y_2O_3$ TBCs. In general, the microhardness of the nitride films is influenced by the surface roughness as well as the hardness of the substrate materials [45]. Since the hardness of the Al_2O_3 substrate was, due to less porosity, higher when compared to zirconia (see section “Analyses and pretreatments of the ceramic substrates”), less pores were exposed by the polishing treatment. This resulted in a more homogenous and denser growth of the PVD films, eventually leading to a higher film hardness of $CrAlSi_{7.5}N$ on alumina as opposed to zirconia.

The microhardness of $Ti_{100\ nm}$/$TiAlSi_{7.9}N$ on nitrided steel was comparable to a former study [18], which examined $TiAlSi_{7.9}N$ as well, despite the fact that no Ti interlayer had been applied. In general, the hardness of the $TiAlSi_{7.9}N$ films was higher than that of $CrAlSi_{7.5}N$ on both the steel and alumina substrate, which can be explained by a high adhesion (Fig. 6), the dense coating growth (Fig. 5(a)), and the stress relaxation effect of the Ti interlayer. Furthermore, small modifications of the stoichiometry, including Si in particular, can decisively affect the mechanical and tribological properties, which was revealed in a further study for the $TiAlSi_{7.9}N$ system [18].

Summary and conclusion

Within this study, the influence of pretreatments such as polishing and plasma etching of thermally sprayed Al_2O_3 and ZrO_2-$8Y_2O_3$ substrates on the surface roughness and the residual stress state was analyzed. Based on the obtained findings, a correlation between the substrate properties and the adhesion as well as the hardness of applied $CrAlSi_{7.5}N$ and $TiAlSi_{7.9}N$ films was established. In particular, the effect of metallic Cr/Ti interlayers on the nitride film adhesion was discussed.

The most significant conclusions drawn from the results of the duplex coatings are summarized as follows:

- Plasma etching of ceramic substrates has no significant impact on the surface roughness, while residual stresses are slightly decreased. In contrast to polished steel substrates, the TBCs exhibited tensile stresses, regardless of a prior polishing or plasma etching.
- Titanium interlayers contribute to the adhesion of $TiAlSi_{7.9}N$ on steel and alumina as Ti compensates compressive and tensile stresses of the substrates. The low or non-existent adhesion of Cr- and Ti-based films on zirconia is assumed to be a result of discrepancies in the lattice structures. Consequently, Cr and Ti exhibit a low chemical affinity towards the oxide ions in ZrO_2-$8Y_2O_3$. In a subsequent study, the ion interchange could be supported by a heat treatment.
- Lower TBC porosities result in a higher microhardness of the applied PVD films due to a smaller number of opened pores on the substrate surface, which evoke coating growth failures, affecting the adhesion and mechanical properties of the PVD films.

Acknowledgements

The authors gratefully thank the DFG (German Research Foundation) within the cooperation project TI 343/122-1 and HO 2356/11-1 (Production and application of graded coating microstructures for the process of friction-spinning using PVD- and thermal spray technology) and the TU Dortmund University within the funding program 'Open Access Publishing' for their financial support.

References

[1] Bemporad E, Sebastiani M, de Felicis D, Carassiti F, Valle R, Casadei F. Production and characterization of duplex coatings (HVOF and PVD) on Ti–6Al–4V substrate. Thin Solid Films 2006;515(1):186–94.
[2] Bemporad E, Sebastiani M, Carassiti F, Valle R. Development of a duplex coating procedure (hvof and pvd) on ti-6al-4v substrate for automotive applications: a collection of papers presented at the 31st international conference on advanced ceramics and composites, January 21–26, 2007. Daytona Beach Florida: Wiley-Interscience; 2009.
[3] Kobayashi A, Yatsuzuka M. Bonding strength of DLC film on zirconia coating prepared by gas tunnel type plasma spraying. Surf Coat Technol 2008;202(24):5914–8.
[4] Bolelli G, Lusvarghi L, Montecchi M, Mantini FP, Pitacco F, Volz H, et al. HVOF-sprayed WC-Co as hard interlayer for DLC films. Surf Coat Technol 2008;203(5–7):699–703.
[5] Bemporad E, Sebastiani M, Staia MH, Puchi Cabrera E. Tribological studies on PVD/HVOF duplex coatings on Ti6Al4V substrate. Surf Coat Technol 2008;203(5–7):566–71.
[6] Chen W, Fang B, Zhang D, Meng X, Zhang S. Thermal stability and mechanical properties of HVOF PVD duplex ceramic coatings produced by HVOF and cathodic vacuum arc. Ceram Int 2017;43:7415–23.
[7] Picas JA, Menargues S, Martin E, Colominas C, Baile MT. Characterization of duplex coating system (HVOF and PVD) on light alloy substrates. Surf Coat Technol 2017;318:326–31.
[8] Zafeiratos S, Kennou S. The interaction of ultrathin nickel films with yttria-stabilized zirconia. Surf Sci 2003;532–535:402–8.
[9] Muñoz MC, Gallego S, Beltrán JI, Cerdá J. Adhesion at metal–ZrO_2 interfaces. Surf Sci Rep 2006;61(7):303–44.
[10] Fessmann J, Grünwald H. Plasma treatment for cleaning of metal parts. Surf Coat Technol 1993;59:290–6.
[11] Ehiasarian AP, Münz W-D, Hultman L, Helmersson U, Petrov I. High power pulsed magnetron sputtered CrNx films. Surf Coat Technol 2003;163–164:267–72.
[12] Schönjahn C, Donohue LA, Lewis DB, Münz W-D, Twesten RD, Petrov I, et al. Enhanced adhesion through local epitaxy of transition-metal nitride coatings on ferritic steel promoted by metal ion etching in a combined cathodic arc/unbalanced magnetron deposition system. J Vacuum Sci Technol 2000;18(4):1718–23.
[13] Barshilia HC, Ananth A, Khan J, Srinivas G. Ar + H2 plasma etching for improved adhesion of PVD coatings on steel substrates. Vacuum 2012;86(8):1165–73.
[14] Schönjahn C, Ehiasarian AP, Lewis DB, New R, Münz W-D, Twesten RD, et al. Optimization of in situ substrate surface treatment in a cathodic arc plasma: a study by TEM and plasma diagnostics. J Vacuum Sci Technol A: Vacuum, Surf Films 2001;19(4):1415–20.
[15] Gerth J, Wiklund U. The influence of metallic interlayers on the adhesion of PVD TiN coatings on high-speed steel. Wear 2008;264(9–10):885–92.
[16] Matthews A, Leyland A. Hybrid techniques in surface engineering. Surf Coat Technol 1995;71(2):88–92.
[17] Kim GS, Lee SY, Hahn JH, Lee BY, Han JG, Lee JH. Effects of the thickness of Ti buffer layer on the mechanical properties of TiN coatings. Surf Coat Technol 2003;171(1–3):83–90.
[18] Tillmann W, Dildrop M. Influence of Si content on mechanical and tribological properties of TiAlSiN PVD coatings at elevated temperatures. Surf Coat Technol 2017;321:448–54.
[19] Gassner M, Schalk N, Sartory B, Pohler M, Czettl C, Mitterer C. Influence of Ar ion etching on the surface topography of cemented carbide cutting inserts. Int J Refract Metal Hard Mater 2017;69:234–9.
[20] Shanmugavelayutham G, Yano S, Kobayashi A. Microstructural characterization and properties of ZrO2/Al2O3 thermal barrier coatings by gas tunnel-type plasma spraying. Vacuum 2006;80(11–12):1336–40.
[21] Limarga AM, Widjaja S, Yip TH. Mechanical properties and oxidation resistance of plasma-sprayed multilayered Al2O3/ZrO2 thermal barrier coatings. Surf Coat Technol 2005;197(1):93–102.
[22] Vogli E, Tillmann W, Selvadurai-Lassl U, Fischer G, Herper J. Influence of Ti/TiAlN-multilayer designs on their residual stresses and mechanical properties. Appl Surf Sci 2011;257(20):8550–7.
[23] Bobzin K. Oberflächentechnik für den Maschinenbau. 1st ed. Weinheim, Germany: Wiley-VCH; 2013.
[24] Menthe E, Rie K-T. Further investigation of the structure and properties of austenitic stainless steel after plasma nitriding. Surf Coat Technol 1999;116–119:199–204.
[25] Chatterjee-Fischer R. Wärmebehandlung von Eisenwerkstoffen: Nitrieren u Nitrocarburieren. Sindelfingen: expert-Verlag; 1986.
[26] Tillmann W, Stangier D, Denkena B, Grove T, Lucas H. Influence of PVD-coating technology and pretreatments on residual stresses for sheet-bulk metal forming tools. Prod Eng Res Dev 2016;10(1):17–24.
[27] Clyne TW, Gill SC. Residual stresses in thermal spray coatings and their effect on interfacial adhesion: a review of recent work. J Therm Spray Technol 1996;5(4):401–18.
[28] Barshilia HC, Ghosh M, Shashidhara Ramakrishna R, Rajam KS. Deposition and characterization of TiAlSiN nanocomposite coatings prepared by reactive pulsed direct current unbalanced magnetron sputtering. Appl Surf Sci 2010;256(21):6420–6.
[29] Mattox DM. Surface effects on the growth, adhesion and properties of reactively deposited hard coatings. Surf Coat Technol 1996;81(1):8–16.
[30] Mittal KL. Adhesion measurement of films & coatings. 2nd ed. The Netherlands: VSP BV; 2001.
[31] Liu M, Ruan H, Zhang L, Moridi A. Effects of misfit dislocation and film-thickness on the residual stresses in epitaxial thin film systems: experimental analysis and modeling. J Mater Res 2012;27(21):2737–45.
[32] Sayir A, Farmer SC. The effect of the microstructure on mechanical properties of directionally solidified $Al_2O_3/ZrO_2(Y_2O_3)$ eutectic. Acta Mater 2000;48:4691–7.
[33] Tillmann W, Dildrop M, Sprute T. Influence of nitriding parameters on the tribological properties and the adhesion of Ti- and Cr-based multilayer designs. Surf Coat Technol 2014;260:380–5.
[34] Hong YS, Kwon SH, Wang T, Kim D-I, Choi J, Kim KH. Effects of Cr interlayer on mechanical and tribological properties of Cr-Al-Si-N nanocomposite coating. Trans Nonferrous Metals Soc China 2011;21:s62–7.
[35] Du H, Zhao H, Xiong J, Xian G. Effect of interlayers on the structure and properties of TiAlN based coatings on WC-Co cemented carbide substrate. Int J Refract Metal Hard Mater 2013;37:60–6.
[36] Pawel JE, McHargue CJ. Use of the scratch test to measure changes in adhesion of Cr/Al2O3 due to ion beam mixing. J Adhes Sci Technol 1988;2(1):385–93.
[37] Bouzakis K-D, Makrimallakis S, Katirtzoglou G, Skordaris G, Gerardis S, Bouzakis E, et al. Adaption of graded Cr/CrN-interlayer thickness to cemented carbide substrates' roughness for improving the adhesion of HPPMS PVD films and the cutting performance. Surf Coat Technol 2010;205(5):1564–70.
[38] Pischow KA, Eriksson L, Harju E, Korhonen AS, Ristolainen EO. The influence of titanium interlayers on the adhesion of PVD TiN coatings on oxidized stainless steel substrates. Surf Coat Technol 1993;58:163–72.
[39] Vassallo E, Caniello R, Cremona A, Dellasega D, Miorin E. Titanium interlayer to improve the adhesion of multilayer amorphous boron carbide coating on silicon substrate. Appl Surf Sci 2013;266:170–5.
[40] Castanho JM, Vieira MT. Improving the cutting performance of TiAlN coatings using submicron metal interlayers. Key Eng Mater 2002;230–232:635–9.
[41] Castanho JM, Pinheiro D, Vieira MT. New multilayer coatings for secondary wood products cutting. Mater Sci Forum 2004;455–456:619–22.
[42] Castanho JM, Vieira MT. Effect of ductile layers in mechanical behaviour of TiAlN thin coatings. J Mater Process Technol 2003;143–144:352–7.
[43] Yang Y, Ong JL, Tian J. Deposition of highly adhesive ZrO2 coating on Ti and CoCrMo implant materials using plasma spraying. Biomaterials 2003;24(4):619–27.
[44] Theunissen GSAM, Bouma JS, Winnubst JAA, Burggraaf AJ. Mechanical properties of ultra-fine grained zirconia ceramics. J Mater Sci 1992;27:4429–38.
[45] Holmberg K, Mathews A. Coatings tribology: a concept, critical aspects and future directions. Thin Solid Films 1994;253(1–2):173–8.